ASTRONAUTIC
TECHNOLOGY DEVELOPMENT

TiungSAT-1 : DATA APPLICATIONS

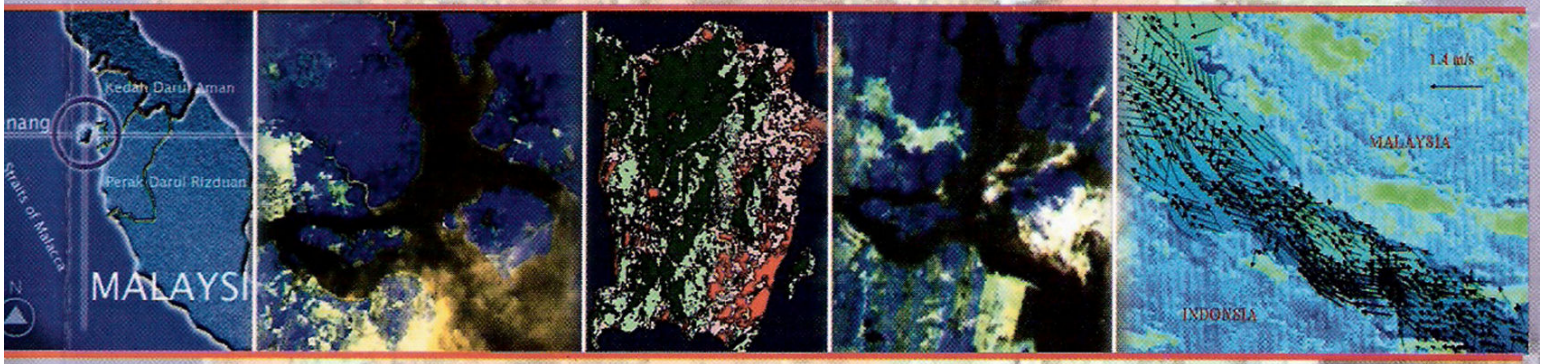

Editors
AHMAD SABIRIN ARSHAD
MAZLAN HASHIM

ATSB

Published by:
Astronautic Technology (M) Sdn. Bhd.

Chapter 7

CLASSIFICATION OF TiungSAT-1 MSEIS DATA FOR LAND COVER MAPPING WITH HYPERSPECTRAL ANALYSIS APPROACH

Alvin Lau Meng Shin and Mazlan Hashim
Department of Remote Sensing
Faculty of Geoinformation Science and Engineering
Universiti Teknologi Malaysia

ABSTRACT

The low to medium spatial resolution satellite data can still be utilized to meet the requirement for a certain level of land cover mapping. However, the land cover classifications of assigning pixel-by-pixel basic to specific land cover classes have been known to be a problematic phenomenon that limits the accuracy of classification. This paper examines the result of utilizing the hyperspectral approach as a recent alternative solution to the above problem to investigate whether or not the sensitivity allowed in the latter can increase the classification accuracy. Using TiungSAT-1 MSEIS data as input, comparative analysis were also performed with classical Maximum Likelihood classification.

The results of this study clearly indicate that hyperspectral analysis can improve classification accuracy of multi-spectral data, especially when the mixed pixels are of great concern.

INTRODUCTION

Land cover information is vital for many planning and management activities. The use of panchromatic, medium-scale aerial photographs to map land cover have been an accepted practice since the 1940s. This was then followed by small scale aerial photographs and satellite images which have been utilized for large area land cover mapping (Lillesand and Kiefer, 1994). Advancement in computer technology and the sensor system for capturing data have enabled finer spatial, spectral and temporal resolution to be achieved. This in turn has influenced the information extraction technique; even in the quantitative approach. The multi-spectral data analysis used to be an optimal quantitative approach for finer spectral resolution satellite data. Recently, the hyperspectral analysis approach was introduced for extracting features from hyperspectral data. The multi-spectral analysis is limited to hyperspectral data. Hence, applying such an approach to classify hyperspectral data has been proven to be futile. On the other hand, if the hyperspectral analysis approach is applied to multi-spectral data classification, will it produce better results? This is the main question to be addressed. In this paper, the hyperspectral data analysis algorithm, namely, the procedural set of extraction features, was examined for classifying TiungSAT-1 MSEIS data - a low spectral (3 bands) and spatial (78 m) resolution multi-spectral data.

In hyperspectral data extraction approach, the concern is not only to label each individual pixel to the anticipated classes but also focus is on the sub-composition of spectra within a pixel for making optimal decisions. The sub-composition of a pixel is a major problem in a statistical-based classification algorithm, and this problem is inevitable in medium-to-low resolution satellite data like TiungSAT-1 MSEIS data.

Compared to the classifiers in recognizing pattern from remotely sensed data, the labeling of a pixel in hyperspectral approach lies within the Spectral Angle Mapper (SAM), where the spectra of every pixel-of-interest and its corresponding reference data were decomposed as vectors, and the angle between them are used for assigning each pixel to a particular class. In other words, this is an automated method for directly comparing image spectra to a known spectra, usually determined in a lab or in the field with a spectrometer known as an endmember. In addition, the SAM is insensitive to illumination

since the SAM algorithm uses only the vector direction and not the vector length. Hence, this forms the hypothesis that SAM could be a more robust classifier even with low spatial resolution data which has high inherent sub-composition of spectra due to large Instantaneous Field of View (IFOV). As a comparative analysis, the widely used Maximum Likelihood algorithm was also applied to classify the same data set.

MATERIALS AND METHODS

Study Area

The study area chosen was Penang Island, (latitudes 5° 30' N to 6° 00' N and longitudes 99° 30' E to 100° 10' E) with a total area of 293 km^2 as shown in Figure 1. About 40% of the study area was a highland area located in the centre with an area of approximately 58.6km^2 and has gazetted as a Reserved Forest (Department of Forestry, Penang). In terms of land cover classes found here included, among others, are the agricultural fields, forest, lakes, industrial area, bare land and urban areas. For the purpose of this study, only five major classes appropriate to spatial resolution of the TiungSAT-1 MSEIS data were established. These classes were: agricultural plantation, industrial area, city and housing area, forest, and water.

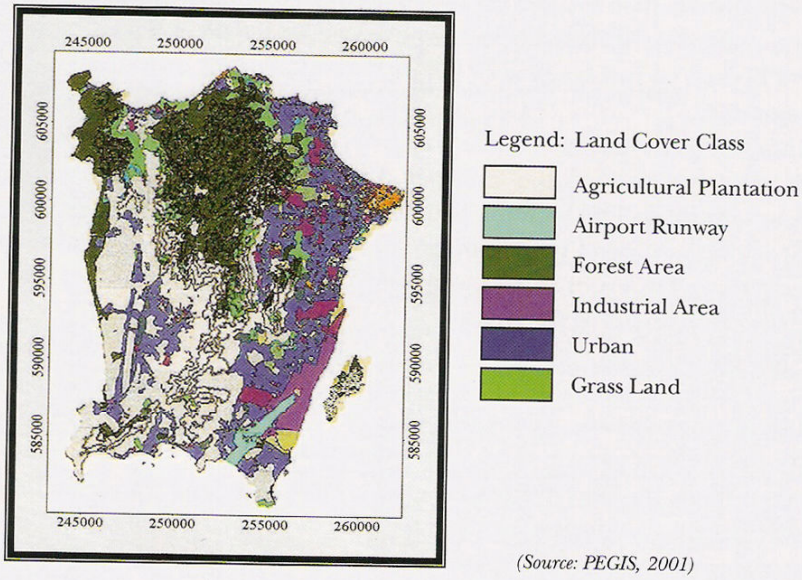

Figure 1. Study Area and its Land Cover Classes

Satellite and Ancillary Data

TiungSAT-1 MSEIS satellite data was used in this study. TiungSAT-1 MSEIS data was categorized as multispectral data with three broad bands: Near Infra-Red (810-890nm), Red (610-690nm) and Green (510-590nm).

The selection of training area was carried out based on the availability of the Land Use map. A total of five classes (industrial area, city and housing area, forest, water and agricultural area) were classified.

Digital Image Processing

The entire digital image processing task in the extraction of land cover information can be divided into four processes: Data Preparation, Pre-Processing, Data Classification and Accuracy Assessment. Figure 2 summarizes the activities undertaken in these four processes.

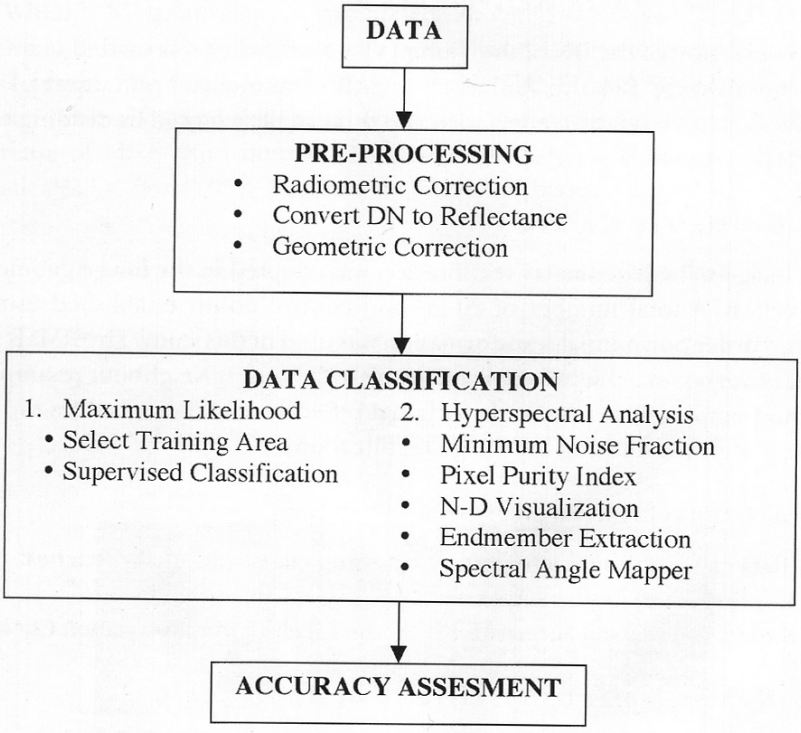

Figure 2. Methodology Employed in Data Processing

Pre-processing

The preprocessing involved three main stages:
(a) Removal of Striping Effect
(b) Conversion of DN to Reflectance
(c) Geometric Correction.

(a) Removal of Striping Effect

TiungSAT-1 MSEIS data used in this study had significant striping effect which needs to be removed before any further processing steps can be performed. This is done in order to remove the unnecessary artifacts and at the same time increase the accuracy of data processing. The Periodic Noise Removal algorithm was used for this purpose, and full explanation can be found in Cannon et al. (1983) and Srinivasan *et al.* (1988).

(b) Convert DN to Reflectance

The conversion of the DN of the TiungSAT-1 MSEIS data was carried out using Internal Average Relative Reflectance (IAR) technique. The output of this conversion is the relative reflectance and this can be achieved by dividing each pixel spectrum by the overall average spectrum.

(c) Geometric Correction

The image-to-map geometry rectification was adopted in the image geometric correction. A total number of 20 ground control points established using a second order polynomial transformation was used in this study. The RMSE *(root mean square)* error achieved was 0.443 pixels with Nearest Neighbour resampling method employed to ensure the original reflectance variation values did not change after performing the image rectification.

Data Classification

The data classifications were performed using classification approaches:
(a) Hyperspectral Analysis Approach
(b) Supervised Classification with Maximum Likelihood Classification Classifier

(a) Hyperspectral Classification Approach

Four steps were carried out in the extraction of land cover classes:
(i) Minimum Noise Fraction
(ii) Pixel Purity Index

(iii) n-D Visualization and Endmembers Extraction
(iv) Classification using Spectral Angle Mapper (SAM).

(i) Minimum Noise Fraction (MNF)

The MNF Transform was applied to further segregate noises thus found in the data (Green et al. 1988). With MNF, the TiungSAT-1 data space was divided into two parts: (1) those with large eigen values and coherent eigen images, and (2) those with near-unity eigen values and noise-dominated images. Both the Eigen values and the MNF images (Eigen images) were used to evaluate the dimensionality of the data. The Eigen values for bands that contain information will be in an order of magnitude larger than those that contain only noise, while the corresponding Eigen images will be spatially coherent. The noise images will not contain any spatial information; but low order magnitude of eigen values. Further explanation of MNF noise removal function can be found in Board and Kruse (1994).

When MNF transform was completed, an eigen value plot (Figure 3) was shown and three MNF-transformed bands (Figure 4) were displayed. From the MNF results, the first two transformed bands (MNF1 and MNF2) contained more information and the spatial coherency decreased significantly with the increase of MNF band number. In MNF bands, the information decreased drastically, i.e. nearly 95% less than the first MNF band.

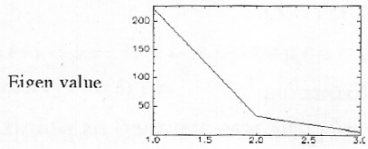

Figure 3. Eigen Values of MNF Transformed Bands Versus Band Number

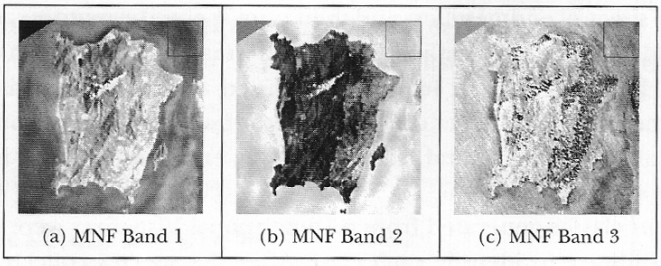

Figure 4: MNF Transformation Bands: (a) MNF Transformed Band 1, (b) MNF Transformed Band 2 and (c) MNF Transformed Band 3

(ii) Pixel Purity Index (PPI)

Within the feature space, the noise-free data occurred as a continuous class from the purest to variety of mixtures. The purest was referred to as endmembers, while mixtures were considered as sub-compositions due to pixels attributes from low to medium resolution of the pixel being recorded. The PPI is a "counting system" to which the number of times each pixel within the scene to be classified are designed as purest. Only MNF Band 1 and MNF Band 2 were selected as input when running PPI. This was because MNF Band 3 with low eigen value only had little information and contained a lot of noise which would decrease the accuracy of the classification result. The results of PPI are shown in Figure 5.

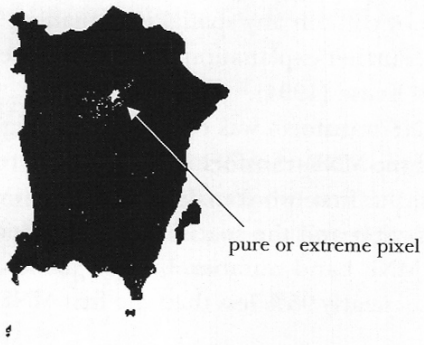

Figure 5. PPI Image

(iii) n-D Visualization and Endmembers Extraction

In this session, TiungSAT-1 data (or spectra) was assumed as points in an n-dimensional scatterplot, where *n* referred to the number of bands. The data for a given pixel corresponded to a spectral reflectance for that given pixel. The distribution of the TiungSAT-1 data in n-space was used to estimate the number of spectral endmembers and their pure spectral signatures and to help understand the spectral characteristics of the materials which make up that signature. Image generated from PPI was used as the input in this session. Spectral library for land cover of study area was built using ROI export from n-D Visualization. Each spectral class (known as endmember) and its spectral profile are shown in Figure 6.

Different classes generated from n-Dimensional Visualizer were compared to spectral library to identify each class. After the spectra collected from n-Dimensional Visualizer were identified, the spectra for each class were saved into a new spectral library file for use during SAM classification.

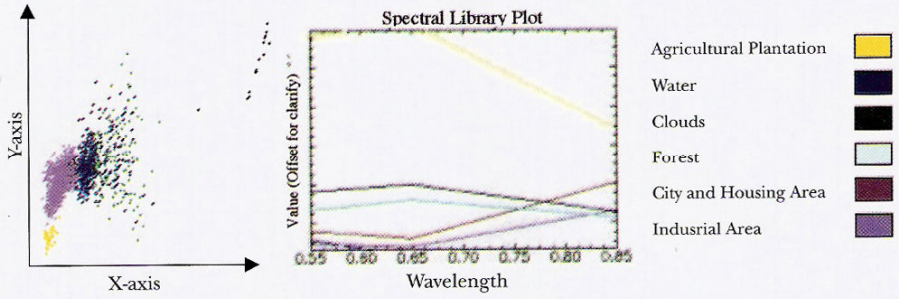

Figure 6. The n-Dimensional Visualizer and spectral class for each endmembers

(iv) Classification using Spectral Angle Mapper (SAM)

The Spectral Angle Mapper (SAM) is an automated method for comparing image spectra to individual spectra or a spectral library (Kruse *et al.*, 1993). The SAM assumes that the data to be classified have been reduced to apparent reflectance. The algorithm determines the similarity between two spectra by calculating the "spectral angle" between them, treating them as vectors in a spectral space with dimensionality equal to the number of bands. A simplified explanation of this can be given by considering a reference spectrum and an unknown spectrum from two-band data. The two different materials will be represented in the 2-D scatter plot by a point for each given illumination, or as a line (vector) for all possible illuminations.

(b) Multi-spectral Approach- Maximum Likelihood Classification

In this study, the Maximum Likelihood Classifier was employed as one of the common widely used classifier to classify the satellite data which later served as comparison to the hyperspectral approach examined in this study. The classification was performed with a supervised approach, where all the three bands are the main feature input using designed training area. The main algorithm used for Maximum Likelihood classification can be found in Jensen (1994).

RESULTS AND DISCUSSION

Classification Result

The classification results of TiungSAT-1 image using Maximum Likelihood Classifier is shown in Figure 7 (a) while classification result using SAM is shown

in Figure 7 (b). The SAM classified image showed an average result and a total of five classes were extracted from the input TiungSAT-1 data.

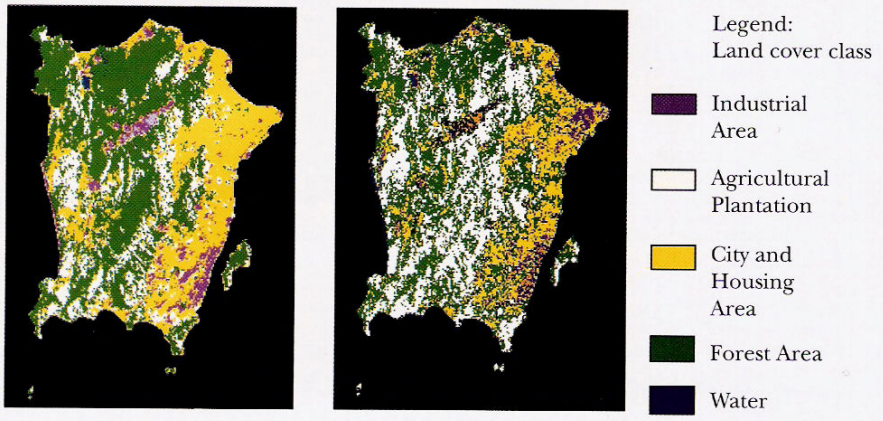

Figure 7. Classification result of TiungSat image using (a) Maximum Likelihood and (b) Spectral Angle Mapper

Accuracy Assessment

Both the classification results from the Maximum Likelihood classification and SAM were compared and analyzed. Digitized land use of the corresponding area was used as ground truth of the classifications. The Kappa statistic was employed in the accuracy assessment.

The SAM classified image achieved overall accuracy of 90% and Kappa coefficient of 0.8 while Maximum Likelihood classified image recorded an overall comparable accuracy of 90% and Kappa coefficient of 0.8. The classification of individual classes for both classified image set was tabulated in Table 1.

It is worth noting that Class 4 and Class 7 (see Table 1) have recorded the least producer accuracy compared to other classes. This is attributed to the TiungSAT-1 MSEIS data that has inadequate spectral characteristic to differentiate these two classes. The forest class gives the best producer accuracy in both classified sets. However, with the limited spectral resolution in TiungSAT-1 MSEIS data, the use of SAM classifier is not advantageous for many similar classes such as Class 5 and Class 7 (see Table 1).

Table 1: Producer and User Accuracy of Each Class for Both Classification

Class*	SAM Classification		Maximum Likelihood Classification	
	Producer Accuracy (%)	User Accuracy (%)	Producer Accuracy (%)	User Accuracy (%)
1	100.00	99.94	100.00	100.00
2	69.43	48.23	42.42	77.42
3	54.60	65.32	59.47	72.90
4	56.83	20.52	42.42	98.57
5	75.57	45.21	93.55	53.64
6	30.20	60.98	47.48	67.62
7	63.52	89.41	47.44	96.32

**Note*: 1= Unclassified, 2=Water, 3=City and Housing Area, 4=Clouds, 5=Forest, 6=Industrial Area, 7=Agricultural Plantation

CONCLUSION

This study has demonstrated that the hyperspectral data classification approach showed a comparable performance in classification accuracy to the classical supervised Maximum Likelihood Classification. With a more robust approach, the SAM classifier skips the tedious training session. With the limitation of spectral band in differentiation of classes in TiungSAT-1 MSEIS data, both classifiers showed comparable results. Apart from the classification results, it was proven that the use of the hyperspectral approach to classify multi-spectral data, was not conducive. This study confirms that hyperspectral analysis does not provide a better approach for the classification of the multi-spectral set. In fact, the limitation within spectral bands input has also persisted in the hyperspectral analysis approach.

ACKNOWLEDGEMENTS

The authors would like to acknowledge the Astronautics Technology (M) Sdn. Bhd. for providing TiungSAT-1 MSES data used in this study.

REFERENCES

Boardman J. W., and Kruse, F. A. 1994. *Automated spectral analysis: A geologic example using AVIRIS data, north Grapevine Mountains, Nevada*: in Proceedings, Tenth Thematic Conference on Geologic Remote Sensing, Environmental Research Institute of Michigan, Ann Arbor, MI.

Cannon, M., Lehar A., and Preston F. 1983. *Background Pattern Removal by Power Spectral Filtering*, Applied Optics, Vol. 22, No. **6**: 777-779.

Jensen, J. R. 1994. *Introductory Digital Image Processing-A Remote Sensing Perspective*, Second Edition, Prentice Hall, Upper Saddle River, New Jersey.

Kruse, F. A., Lefkoff, A. B., Boardman, J. W., Heidebrecht, K. B., Shapiro, A. T., Barloon, J. P., and Goetz, A. F. H. 1993. *The spectral image processing system (SIPS) - Interactive visualization and analysis of imaging spectrometer data*, Remote Sensing of Environment, v. 44, 145 - 163.

Lillesand, T.M. and Kiefer, R.W. 1999. *Remote Sensing and Image Interpretation*, Forth Edition, John Wiley and Son, New York.

Penang Geographical Information System (PEGIS) Centre. 2001. web address: http://pegismap.sukpp.gov.my/webpegis/index.htm.

Srinivasan, Ram, Cannon M., and White J. 1988. *Landsat Data Destriping Using Power Spectral Filtering*, Optical Engineering, Vol. 27, No. 11: 939-943.